2016 European Control Conference (ECC)
June 29 - July 1, 2016. Aalborg, Denmark

Distributed Predictive Control Approach for Fuel Efficient Gear Shifting in Hybrid Electric Vehicles

Martina Joševski and Dirk Abel

Abstract— **Energy management strategies (EMS) employed in hybrid electric vehicles determine the toque split between propulsion machines in such a way that the driver torque demand is satisfied. Therefore, a certain cost function is minimized over a driving cycle subject to constraints on the powertrain. Apart from optimizing the torque distribution the EMS can consider the optimization of clutch engagement and gear choice to further improve the overall fuel economy of the hybrid system. This paper presents a distributed predictive control architecture in which one control module computes the fuel optimal sequence of torque distributions while the other control entity determines the fuel optimal sequence of gear shift commands. To formulate the distributed control problem, the original mixed-integer optimal control problem is reformulated using partial outer convexification and relaxation. The fuel performance and computational complexity are evaluated in comparison to a centralized mixed-integer model predictive controller. Simulation results on a real-world driving cycle show that while nearly the same fuel economy is achieved, significant computational asset is gained with the distributed predictive controller being able to be executed on a rapid control prototyping platform.**

I. INTRODUCTION

Advanced control strategies for hybrid electric vehicles (HEVs) are commonly designed to comply with various objectives simultaneously such as improving the fuel economy, reducing the emission of harmful gases and improving the overall vehicle comfort and drivability. Regarding vehicle drivability, the frequency of engine start-stop events, the gear switching events and the time needed to deliver the torque requested by the driver at the wheels are some of the factors which are commonly addressed and investigated [1]–[5]. All these subjects can be addressed in a single algorithm running on a centralized electronic control unit (ECU). However, in a common passenger vehicle algorithms are usually executed on different ECUs to achieve a modular, flexible and cost-optimized architecture, e.g., the engine is controlled by the engine ECU while gear shifts are optimized by the gearbox ECU. While the global optimal solution might only be obtained in a centralized optimization, a sub-optimal solution can be gained in a distributed control scheme in which the local controllers interact by exchanging state and control input trajectories.

If the hybrid vehicle is equipped with an automatic transmission an optimal generation of the gear trajectory further improves the overall fuel economy of the hybrid system. Some of the optimization based approaches for the gear shifting, introduced earlier in literature, can be found in [6], [7]. In [6] the authors used dynamic programming (DP) to derive the optimal trajectories of the power split and gear choices with regards to a cost function incorporating the integral fuel consumption and emissions over the driving cycle. In [4] a method based on the combination of dynamic programming (DP) and Pontryagins minimum principle (PMP) is developed. The method consists of deriving the optimal engine power based on PMP in the inner loop while the gear shifts, are optimally controlled by using DP in the outer loop. The approach presented in [7] relies on a mixed-integer linear program which includes the power split, gear and clutch control.

A. Main Contribution

In this work we introduce a distributed predictive energy management concept to control the torque distribution and gear shifting of a parallel hybrid electric vehicle over a driving cycle. The energy management problem is solved by decomposing it into two control units: one responsible for generating the fuel optimal sequence of torque distributions and the other one which computes the fuel optimal gear choice trajectory. Both controllers are realized as model predictive control (MPC) schemes. Thereby the MPC controller for the torque distribution is based on a linear time-varying MPC (LTV-MPC) approach while the gear shifting controller solves a MPC problem which can be solved efficiently. To define the distributed control architecture the original nonlinear mixed-integer optimal control problem is approximated using partial outer convexification and relaxation [8], [9] for the gear choices. Thereby the outer convexification defines binary control functions for the integer choices. The reformulation leads to a binary convexified nonlinear program. In the distributed MPC scheme the binary controls are additionally relaxed to define the optimization problem for the gear shifting. Relaxation leads to the formulation of a quadratic optimal control problem which can be solved efficiently by applying mature quadratic programming (QP) solvers. The distributed arrangement enables real-time capable optimization and corresponds to a usually applied vehicle architecture. Furthermore the distributed EMS is realized as a cooperative MPC procedure in which both controllers optimize the same goal, i.e., the fuel consumption rate and battery usage over a driving mission. The simulation results when the distributed control architecture is employed are compared to the results when the centralized MPC controller

The research is funded by German Scientific Foundation (Deutsche Forschungsgemeinchaft (DFG)). The grant is thankfully acknowledged.

M.Joševski and D. Abel are with the Institute of Automatic Control, Department of Mechanical Engineering, RWTH Aachen University, 52074 Aachen, Germany, {M.Josevski, D.Abel}@irt.rwth-aachen.de

is utilized. The computational complexity is significantly reduced when the controls are determined in a distributed control scheme.

The contribution is organized as follows. In section II the HEV model which is subsequently applied to design the controller is introduced. The centralized MPC approach is presented in section III, while in section IV the distributed MPC concept is detailed. Section V clarifies the simulation setup and discusses the simulation results for both concepts. Finally, section VI provides a brief overview of the paper subject and gives implications for future work.

II. Vehicle Model

In this work we investigate a parallel hybrid vehicle topology. We assume that the internal combustion engine (ICE) and the electric machine (EM) are mechanically coupled and that a battery pack is applied as an energy buffer. The gearbox is realized as an automatic five-stage transmission. Assuming that ICE and EM are connected through a torque coupler, the mechanical coupling equation:

$$T_{wh,req} = \begin{cases} \eta_{gb} R_{gb}(\gamma^j)(T_{ice} + T_{em}) - T_{br}, & T_{gb} \geq 0 \\ \frac{1}{\eta_{gb}} R_{gb}(\gamma^j)(T_{ice} + T_{em}) - T_{br}, & T_{gb} < 0 \end{cases} \quad (1)$$

with $j \in \{1, \ldots, n_g\}$ is satisfied at every time instant t, where $T_{wh,req}$ is the wheel torque request assigned by the driver, $T_{gb} = T_{ice} + T_{em}$ the gearbox torque at the input stage, η_{gb} the transmission efficiency, $R_{gb}(\gamma^j)$ the transmission ratio for the gear γ^j, n_g the number of discrete gear choices, while T_{ice}, T_{em} and T_{br} correspondingly define the ICE, EM torque and the torque of the friction brakes. The parameters of the vehicle are adopted from the simulation software ADVISOR [10]. The dynamics faster than 1 Hz are neglected due to the sample rate of the used controllers. Therefore the transient responses of the engine and the motor are not part of the HEV system model. Instead the propulsion machines are represented by quasi-static nonlinear functions.

As a part of the HEV model, which is commonly considered when the energy management controller is designed, the longitudinal vehicle velocity and the state of charge (SoC) dynamics are applied as system states.

1) Vehicle Dynamics: For the longitudinal vehicle dynamics the following relation holds:

$$\dot{v} = \frac{1}{m}\left(\frac{T_{wh}}{r_{wh}} - m\,g\,f_r\,cos\theta - m\,g\,sin\theta - \frac{1}{2}\,c_d\,A\,\rho\,v^2\right) \quad (2)$$

where v represents the velocity of the vehicle, θ is the road inclination, ρ is the air density, c_d is the drag coefficient, A is the vehicles cross section, f_r is the rolling resistance coefficient, m is the vehicle mass including the mass of the load.

2) Battery Dynamics and Electric Motor: The battery dynamics are commonly represented by the dynamics of its state of charge. When the well known equivalent electric circuit model [11] of the battery is applied the SoC dynamics are given by:

$$\dot{SoC} = -\frac{U_{oc} - \sqrt{U_{oc} - 4R_{int}P_{em}}}{2R_{int}Q_{batt}} \quad (3)$$

where Q_{batt} denotes the battery capacity, U_{oc} is the open circuit voltage, R_{int} the internal resistance while P_{em} represents the terminal electric power supplied to or generated by the motor. In this work we represent P_{em} by a polynomial function of the EM angular speed ω_{em} and torque T_{em}:

$$P_{em}(T_{em}, \omega_{em}) \approx \sum_{i=0}^{3}\sum_{j=0}^{3} a_{ij} \cdot \omega_{em}^i \cdot T_{em}^j \quad (4)$$

Constraints on electric machine speed and electric torque are defined as:

$$0 \leq \omega_{em} \leq \omega_{em,max} \quad (5)$$

$$T_{em,min}(\omega_{em}) \leq T_{em} \leq T_{em,max}(\omega_{em}) \quad (6)$$

3) Engine and Fuel Consumption: As the optimization of the HEV fuel efficiency is an essential aim of the HEV energy management strategy, the fuel consumption rate is defined as a controlled output. In this regard, the fuel consumption rate is represented as:

$$\dot{m}_f(T_{ice}, \omega_{ice}) \approx \sum_{i=0}^{3}\sum_{j=0}^{3} b_{ij} \cdot \omega_{ice}^i \cdot T_{ice}^j \quad (7)$$

where ω_{ice} and T_{ice} stand for the ICE angular speed and torque respectively. Constraints on the engine speed and engine torque are:

$$\omega_{ice,min} \leq \omega_{ice} \leq \omega_{ice,max} \quad (8)$$

$$0 \leq T_{ice} \leq T_{ice,max}(\omega_{ice}) \quad (9)$$

Assuming the clutch to be closed, the following relations hold for the engine and motor angular speed:

$$\omega_{ice} = \omega_{em} \quad (10)$$

$$\omega_{em} = \omega_{wh} R_{gb}(\gamma^j) = \frac{v}{r_{wh}} R_{gb}(\gamma^j) \quad (11)$$

where w_{wh} represents the wheel angular velocity while r_{wh} denotes the wheel radius.

III. Centralized Mixed-Integer MPC Scheme

As both continuous (i.e. ICE power/torque, EM power/torque) and discrete control inputs (i.e. the gear choice) appear in the formulation of the optimal control problem (OCP), the OCP of the HEV energy management strategy falls into the group of *Mixed-Integer OCP (MIOCP)*. To approach MIOCP various techniques have been proposed, among them those based on enumeration (full enumeration, dynamic programming), branching techniques (branch & bound, branch & cut), outer approximation and reformulations (convexification and relaxation). A comprehensive overview of techniques applied to solve MIOCP can be found in [8]–[12]. In order to develop an EMS strategy which tackles the problem of gear shifting, we apply the partial outer convexification to reformulate the original MIOCP for the HEV fuel optimization. Furthermore we formulate a distributed predictive control scheme, in which the torque split and the gear shifting are optimized separately, see section IV. However both MPCs determine

a corresponding control sequence with respect to the same performance index, i.e., both controllers optimize the fuel consumption and battery usage over the prediction horizon and thus act in a cooperative way. Convexification and relaxation approaches [8] aim at reformulating the original optimization problem as a purely continuous nonlinear program (NLP) for which computationally highly efficient solution methods exist and are presented in the sequel of this contribution. The term convexification in the following refers to a convex reformulation of the dynamics and later also of the constraints with respect to the integer controls. All other parts of the discretized optimal control problem remain untouched and hence possibly nonlinear and/or non-convex.

A. Centralized Benchmark Controller

1) Mixed-Integer Prediction Model: As a benchmark controller a centralized MPC scheme is realized in which both, gear changes and torque distribution between the ICE, EM and the friction brakes are simultaneously optimized in such a way that the fuel consumption is minimized and the propulsion machines as well as the energy storage are kept within their respective operational bounds. The nonlinear HEV model for the centralized MPC is derived from (1)-(4), (7):

$$\dot{x}(t) = f(x(t), u(t), \gamma^j(t), z(t)) \tag{12}$$

$$y(t) = g(x(t), u(t), \gamma^j(t)) \tag{13}$$

$\forall j \in \{1, \ldots, n_g\}$, where $x = \begin{bmatrix} v & SoC \end{bmatrix}^T$ represents the state vector, $u = \begin{bmatrix} T_{ice} & T_{br} \end{bmatrix}^T$ are the continuous control inputs, γ^j are integer control inputs (gear choices) from the discrete set $\mathcal{G} = \{\gamma^1, \ldots, \gamma^{n_g}\}$, $z = T_{wh,req}$ is the driver torque request which acts as an exogenous disturbance while $y = \begin{bmatrix} \dot{m}_f & SoC \end{bmatrix}^T$ is the vector of controlled outputs. Although T_{em} is not part of the vector of control inputs, it can be derived from u and z in accordance to (1). In order to design a centralized MPC controller in addition to the continuous control inputs, which refer to the torque distribution, discrete control inputs for the individual gear options have to be determined as well.

2) Outer Convexification: For optimization, we transform the model (12)-(13) to its convexified counterpart using outer convexification as proposed in [8]–[13]. In this way, we obtain a computational speedup of several orders of magnitude while being still close to the optimal solution, see [14]. Furthermore, we are able to apply mature solvers to gain a solution of the convexified mixed-integer problem. Particularly, we obtain our model in the following form:

$$\dot{x}(t) = \sum_{j=1}^{n_g} \gamma_j(t) f(x(t), u(t), \gamma^j, z(t)) \tag{14}$$

$$y(t) = \sum_{j=1}^{n_g} \gamma_j(t) g(x(t), u(t), \gamma^j) \tag{15}$$

The idea of the outer convexification, as proposed in [8]–[13] is to introduce binary control functions $\gamma_j(t) \in \{0, 1\}$, $1 \leq j \leq n_g$ which indicate if the discrete choice γ^j is active at time t. Thereby the binary control functions fulfill the *Special Order Set Property (SOS-1)* according to the following definition.

Definition 1 (Special Order Set Property Type-1)
We say that the variables $(\gamma_1, \ldots, \gamma_{n_g})$ fulfill the special order set type one property if they satisfy the following relation:

$$\sum_{j=1}^{n_g} \gamma_j(t) = 1, \qquad \gamma_j(t) \in \{0, 1\},\ 1 \leq j \leq n_g \tag{16}$$

In order to formulate the centralized energy management problem, we evaluate our continuous-time convexified model (14)-(15) at equidistant discrete time instances t_k and solve the differential equations by numerical integration. Thus, a finite-dimensional optimization problem is gained. In the following the notation $\{\cdot\}_{k+j|k}$ refers to the value of variable $\{\cdot\}$ at time t_{k+j} along the prediction horizon when the current time is t_k.

3) Optimal Control Problem: For our energy management problem, the quadratic performance index:

$$\begin{aligned} J = &\sum_{i=1}^{H_p} \|y_{k+i|k} - y_{ref}\|_Q^2 + \sum_{i=0}^{H_u-1} \|\Delta u_{k+i|k}\|_{R_u}^2 \\ &+ \sum_{i=0}^{H_u-1} \|\Delta \gamma_{k+i|k}\|_{R_\gamma}^2 + \sum_{i=0}^{H_u-1} \|u_{k+i|k}\|_S^2 + \rho_s \epsilon_s \end{aligned} \tag{17}$$

is minimized subject to system dynamics (14)-(15), SOS-1 constraints:

$$\textstyle\sum_{j=0}^{n_g} \gamma_{j,k+i|k} = 1, \quad \gamma_{j,k+i|k} \in \{0, 1\}, \quad \gamma^j_{k+i|k} \in \mathcal{G} \tag{18}$$

for $0 \leq i \leq H_u - 1$, SoC constraints:

$$SoC_{min} - \epsilon_s \leq SoC_{k+i|k} \leq SoC_{max} + \epsilon_s \tag{19}$$

for $1 \leq i \leq H_p$, constraints related to the ICE and EM angular speed:

$$\textstyle\sum_{j=1}^{n_g} \gamma_{j,k+i|k} \cdot \omega_{ice,k+i|k}(\gamma^j_{k+i|k}) \leq \omega_{ice,max} \tag{20}$$

$$\textstyle\sum_{j=1}^{n_g} \gamma_{j,k+i|k} \cdot \omega_{ice,k+i|k}(\gamma^j_{k+i|k}) \geq \omega_{ice,min} \tag{21}$$

$$\textstyle\sum_{j=1}^{n_g} \gamma_{j,k+i|k} \cdot \omega_{em,k+i|k}(\gamma^j_{k+i|k}) \leq \omega_{em,max} \tag{22}$$

$$\textstyle\sum_{j=1}^{n_g} \gamma_{j,k+i|k} \cdot \omega_{em,k+i|k}(\gamma^j_{k+i|k}) \geq \omega_{em,min} \tag{23}$$

for $0 \leq i \leq H_p$ as well as the constraints related to the ICE and EM minimum and maximum torque:

$$T_{ice,k+i|k} \leq \textstyle\sum_{j=1}^{n_g} \gamma_{j,k+i|k} \cdot T_{ice,max}(\gamma^j_{k+i|k}) \tag{24}$$

$$T_{ice,k+i|k} \geq \textstyle\sum_{j=1}^{n_g} \gamma_{j,k+i|k} \cdot T_{ice,min}(\gamma^j_{k+i|k}) \tag{25}$$

$$T_{em,k+i|k} \leq \textstyle\sum_{j=1}^{n_g} \gamma_{j,k+i|k} \cdot T_{em,max}(\gamma^j_{k+i|k}) \tag{26}$$

$$T_{em,k+i|k} \geq \textstyle\sum_{j=1}^{n_g} \gamma_{j,k+i|k} \cdot T_{em,min}(\gamma^j_{k+i|k}) \tag{27}$$

$$T_{br,k+i|k} \geq 0, \tag{28}$$

for $0 \leq i \leq H_u - 1$. In (20)-(23), we have to define $\gamma_{j,k+i|k} = \gamma_{j,k+H_u-1|k}$ and $\gamma^j_{k+i|k} = \gamma^j_{k+H_u-1|k}$ for $i \geq H_u$

as the control inputs remain constant at the end of the control horizon. The performance index (17) embraces the summation terms over the prediction horizon of the length H_p and the control horizon of the length H_u respectively. The first term of the quadratic cost weights the deviation of the fuel consumption rate $\dot{m}_f$ and the SoC from their corresponding reference values, being zero for $\dot{m}_f$ and constantly SoC_{ref} for SoC. The second term penalizes the T_{ice} and T_{br} changes over the prediction horizon where $\Delta u_{k+j|k} = u_{k+j|k} - u_{k+j-1|k}$. In this way we achieve smooth transitions of the continuous control inputs. In addition frequent gear switching is avoided by introducing the third term in the quadratic cost where $\Delta\gamma_{k+j|k} = \gamma_{k+j|k} - \gamma_{k+j-1|k}$. However, this term does not penalize non-sequential gear shifts, e.g., switching from gear 2 to 4 but weights the decision to change the current gear. Finally the absolute values of the control inputs are penalized in order to accomplish that the braking torque is used only in situations when it is not possible to recuperate the kinetic energy. It has to be noticed that the upper and lower bounds on T_{ice} and T_{em} change in dependence on their respective angular velocities ω_{ice} and ω_{em}. The constraints on the battery SoC are imposed in accordance with operational limits introduced by the manufacturer of the battery pack. To guarantee the feasibility of the optimization problem the SoC constraints are implemented as soft constraints using the the slack variable ϵ_s. The entire optimization problem including (14)-(15), (17)-(28) is solved as a sequential mixed-integer quadratic program. In this regard, the performance index (17) as well as and the nonlinear constraints which refer to the system dynamics (14)-(15), SoC constraints (19) and T_{em} constraints (26)-(27) are linearized along the prediction horizon. The remaining constraints are already expressed in a linear form. The weighting matrices are defines as: $Q = diag(q_{\dot{m}_f}, q_{SoC})$, $R_u = diag(r_{\Delta T_{ice}}, r_{\Delta T_{br}})$, $R_\gamma = diag(r_{\Delta\gamma_1}, \ldots, r_{\Delta\gamma_{n_g}})$ and $S = diag(s_{T_{ice}}, s_{T_{br}})$. When the optimal control sequence $u^*_{k|k}, \gamma^*_{k|k}, \ldots, u^*_{k+H_u-1|k}, \gamma^*_{k+H_u-1|k}$ is obtained only the elements corresponding to the first time instant are applied to the HEV powertrain. Therefore the binary controls $\gamma^*_{1,k|k}, \ldots, \gamma^*_{n_g,k|k}$ are mapped to the corresponding integer solution $\gamma^{j,*}_{k|k}$.

IV. Distributed Cooperative MPC Scheme

Figure 1 shows the general structure of the distributed control approach. Both controllers receive the estimated future requested torque sequence as well as the information on the current HEV system states. In addition, both controllers interact by exchanging their local (predicted) state and control input trajectories. Using the local trajectories of the torque split MPC, the gear shifting MPC optimizes the selection of appropriate gears over the prediction horizon. This optimal gear trajectory is then transmitted to the MPC controller which determines the torque distribution that is applied to the HEV powertrain. In addition, both controllers act on the same time scale.

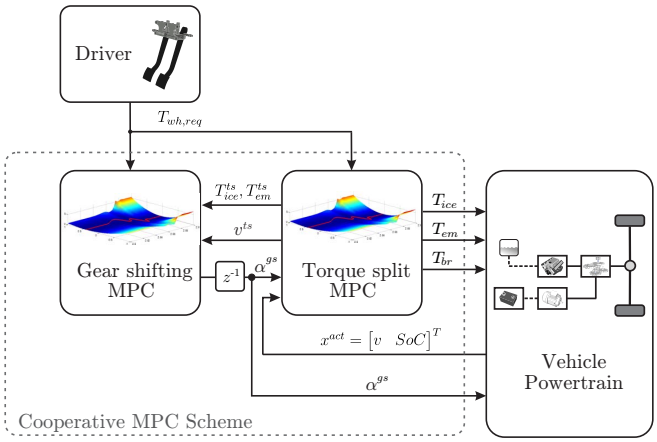

Fig. 1. Structure of the Distributed Cooprative MPC Scheme

A. Torque Split MPC

The goal of this MPC scheme is to determine the torque distribution between the propulsion machines in such a way that the fuel economy is optimized and the hybrid powertrain is maintained within its operational limits.

1) Continuous Prediction Model: The nonlinear HEV model of the MPC which determines the sequence of torque distributions is derived from (1)-(4), (7) and can be summarized as:

$$\dot{x}(t) = f(x(t), u(t), z(t)) \tag{29}$$
$$y(t) = g(x(t), u(t), z(t)) \tag{30}$$

where $x = \begin{bmatrix} v & SoC \end{bmatrix}^T$ represents the state vector, $u = \begin{bmatrix} T_{ice} & T_{br} \end{bmatrix}^T$ the control input vector, $z = \begin{bmatrix} T_{wh,req} & \gamma^{gs} \end{bmatrix}^T$ is the exogenous disturbance vector and $y = \begin{bmatrix} \dot{m}_f & SoC \end{bmatrix}^T$ the vector of controlled outputs. Particularly the disturbance vector z is composed of the requested driver torque $T_{wh,req}$ and the gear sequence γ^{gs} originating from the gear shifting optimizer. The MPC is realized as a linear time-varying MPC scheme and therefore the system dynamics (29)-(30) are linearized at every time instant k which results in the following discrete time state space representation:

$$x_{k+1} = A_k x_k + B_k u_k + W_k z_k + \Gamma_k \tag{31}$$
$$y_k = C_k x_k + D_k u_k + V_k z_k + \Pi_k \tag{32}$$

where $A_k \in \mathbb{R}^{2\times2}$ denotes the system matrix, $B_k \in \mathbb{R}^{2\times2}$ the input matrix, $C_k \in \mathbb{R}^{2\times2}$ the output matrix, $W_k \in \mathbb{R}^{2\times2}$ and $V_k \in \mathbb{R}^{2\times2}$ describe the influence of the system disturbance w on the states and outputs respectively and $\Gamma_k \in \mathbb{R}^{2\times1}$ as well as $\Pi_k \in \mathbb{R}^{2\times1}$ indicate affine terms that result from the linearization at the current operating point.

2) Optimal Control Problem: In order to obtain an optimal sequence of torque distributions the following optimiza-

tion problem is solved:

$$\min_{\Delta u_{(\cdot|k)},\epsilon_s} \sum_{i=1}^{H_p} \|y_{k+i|k} - y_{ref}\|^2_{Q_{ts}} + \sum_{i=0}^{H_u-1} \|\Delta u_{k+i|k}\|^2_{R_{ts}} + \sum_{i=0}^{H_u-1} \|u_{k+i|k}\|^2_{S_{ts}} + \rho_s \epsilon_s \tag{33}$$

subject to the discrete system dynamics (31)-(32), constraints associated with the ICE and EM minimum and maximum torque:

$$T_{ice,k+i|k} \leq T_{ice,max}(\omega_{ice,k+i|k}) \tag{34}$$
$$T_{ice,k+i|k} \geq T_{ice,min}(\omega_{ice,k+i|k}) \tag{35}$$
$$T_{em,k+i|k} \leq T_{em,min}(\omega_{em,k+i|k}) \tag{36}$$
$$T_{em,k+i|k} \geq T_{em,max}(\omega_{em,k+i|k}) \tag{37}$$
$$T_{br,k+i|k} \geq 0, \tag{38}$$

with $0 \leq i \leq H_u - 1$ as well as the state constraints:

$$SoC_{max} - \epsilon_s \leq SoC_{k+i|k} \leq SoC_{max} + \epsilon_s \tag{39}$$
$$\epsilon_s \geq 0, \tag{40}$$

with $1 \leq i \leq H_p$. In this context, the terms of the cost function correspond to those of the centralized optimization problem introduced in section III-A.3. The weighting matrices of the performance index (33) are introduced as follows: $Q_{ts} = diag(q^{ts}_{\dot{m}_f}, q^{ts}_{SoC})$, $R_{ts} = diag(r^{ts}_{\Delta T_{ice}}, r^{ts}_{\Delta T_{br}})$ and $S_{ts} = diag(s^{ts}_{T_{ice}}, s^{ts}_{T_{br}})$. When the optimal control sequence $\Delta u^*_k = [\Delta u^*_{k|k}, \ldots, \Delta u^*_{k+H_u-1|k}]$ is obtained only the first computed element is applied to calculate the control action which is applied to the plant. In addition the T_{em} and T_{ice} trajectories are computed by:

$$T_{ice,k+i|k} = T_{ice,k|k} + \sum_{m=0}^{i} \Delta T_{ice,k+m|k} \tag{41}$$

$$T_{em,k+i|k} = T_{em,k|k} + \sum_{m=0}^{i} \Delta T_{em,k+m|k}, \tag{42}$$

for $0 \leq i \leq H_u$-1 which together with the state trajectories, i.e. v and SoC trajectories, are submitted to the gear shifting controller.

B. Gear Shifting MPC

In the distributed cooperative MPC scheme both MPC agents minimize the same performance index. Hence the gear shifting MPC controller determines the gear sequence such that the fuel consumption rate and the SoC deviation from its reference value are minimized over the prediction horizon. The gear shifting MPC controller is realized by solving a constrained quadratic predictive control problem.

1) Convexified and Relaxed Prediction Model: In order to formulate the predictive OCP the original binary controls $\gamma_j, 1 \leq j \leq n_g$ are additionally replaced by the relaxed counterparts $\alpha_j(t) \in [0,1] \subset \mathbb{R}$. To simplify notation we subsequently introduce integer variables $\alpha^j \in \mathcal{G}, 1 \leq j \leq n_g$ which are defined in the same fashion as $\gamma^j \in \mathcal{G}, 1 \leq j \leq n_g$ in section III-A.1, i.e., they denote the particular gear choice realization. Like the binary controls, the relaxed controls are imposed to the SOS-1 type constraints. For the gear shifting controller we apply the following convexified and relaxed model:

$$\dot{x}(t) = \sum_{j=1}^{n_g} \alpha_j(t) f(\alpha^j, z(t)) \tag{43}$$

$$y(t) = \sum_{j=1}^{n_g} \alpha_j(t) g(\alpha^j, z(t)) \tag{44}$$

where $x = SoC$ denominates the state of the examined system, $y = \begin{bmatrix} \dot{m}_f & SoC \end{bmatrix}^T$ are the controlled outputs, $\alpha = \begin{bmatrix} \alpha_1, \ldots, \alpha_{n_g} \end{bmatrix}^T \in [0,1]^{n_g} \subset \mathbb{R}^{n_g}$ denotes the vector of control variables while $z = \begin{bmatrix} T_{wh,req} & z^{ts} \end{bmatrix}^T$ with $z^{ts} = \begin{bmatrix} T^{ts}_{ice} & T^{ts}_{em} & v^{ts} \end{bmatrix}^T$ is the augmented disturbance vector. The disturbance vector comprises the driver torque demand trajectory $T_{wh,req}$ as well as the state and input trajectories obtained from the torque distribution controller, i.e., the T^{ts}_{ice}, T^{ts}_{em} and v^{ts} trajectories respectively. Although, the angular speeds ω_{ice} and ω_{em} of the propulsion machines can unambiguously be determined in dependence of the transmission ratio $R_{gb}(\alpha^j)$ in gear α^j, the torque distribution after shifting that fulfills the driver torque demand is unknown. Assuming (as a best guess) that the power of the propulsion machines remains constant when shifting from gear α^i to gear α^j, i.e.,

$$R_{gb}(\alpha^i) \frac{v^{ts}}{r_{wh}} T_{ice/em} = R_{gb}(\alpha^j) \frac{v^{ts}}{r_{wh}} \lambda_s T_{ice/em} \tag{45}$$

where $T_{ice/em}$ denotes the ICE / EM torque in gear α^i, we obtain the torque scaling factor λ_s as

$$\lambda_s(\alpha^i, \alpha^j) = \frac{R_{gb}(\alpha^i)}{R_{gb}(\alpha^j)}. \tag{46}$$

Thus, we can derive the torque in gear α^j as $\lambda_s(\alpha^i, \alpha^j)\, T_{ice/em}$. Similar to the centralized scheme, we evaluate the continuous time variables at equidistant discrete time steps. In the following we replace the continuous time notation t_{k+i} with the corresponding index $k + i$ which refers to the evaluation of the respective continuous function at time step t_{k+i}.

2) Optimal Control Problem: The controller solves the following optimization problem at every time step:

$$\min_{\alpha_{(\cdot|k)}} \sum_{i=1}^{H_p} \|y_{k+i|k} - y_{ref}\|^2_{Q_{gs}} + \sum_{i=0}^{H_u-1} \|\Delta \alpha_{k+i|k}\|^2_{R_{gs}} \tag{47}$$

subject to the following constraints:

$$x_{k+i+1} = \sum_{j=1}^{n_g} \alpha_{j,k+i}\, f(\alpha^j_{k+i}, z_{k+i}) \tag{48}$$

$$y_{k+i+1} = \sum_{j=1}^{n_g} \alpha_{j,k+i}\, g(\alpha^j_{k+i}, z_{k+i}) \tag{49}$$

$$\sum_{j=1}^{n_g} \alpha_{j,k+i} = 1,\ \alpha_{j,k+i} \in [0,1],\ 1 \leq j \leq n_g \tag{50}$$

where $0 \leq i \leq H_u - 1$, $\Delta\alpha_{j,k+i} = \alpha_{j,k+i} - \alpha_{j,k+i-1}$ while the weighting matrices are defined as $Q_{gs} = diag(q^{gs}_{\dot{m}_f}, q^{gs}_{SoC})$ and $R_{gs} = diag(r^{gs}_{\Delta\alpha_1}, \ldots, r^{gs}_{\Delta\alpha_{n_g}})$. While the first term of the cost function is equivalent to that of the torque distribution controller, the second term weights the change of relaxed control inputs in order to prevent the controller from frequent gear switching. Thereby the change of the respective gear is penalized. Again, we have to define $\alpha_{j,k+i|k} = \alpha_{j,k+H_u-1|k}$ and $\alpha^j_{k+i|k} = \alpha^j_{k+H_u-1|k}$ for $i \geq H_u$ as the control inputs remain constant at the end of the control horizon.

3) Excluding Infeasible Solutions: Based on the velocity and torque trajectories obtained from the torque distribution MPC, we prove the feasibility of each relaxed control before the optimization to additionally increase the computational efficiency. It is analyzed if the following inequalities regarding the ICE and EM angular velocities:

$$R_{gb}(\alpha^j_{k+i|k}) \frac{v^{ts}_{k+i|k}}{r_{wh}} \leq \omega_{ice,max} \tag{51}$$

$$R_{gb}(\alpha^j_{k+i|k}) \frac{v^{ts}_{k+i|k}}{r_{wh}} \geq \omega_{ice,min} \tag{52}$$

$$R_{gb}(\alpha^j_{k+i|k}) \frac{v^{ts}_{k+i|k}}{r_{wh}} \leq \omega_{em,max} \tag{53}$$

$$R_{gb}(\alpha^j_{k+i|k}) \frac{v^{ts}_{k+i|k}}{r_{wh}} \geq \omega_{em,min} \tag{54}$$

for $0 \leq i \leq H_p, 1 \leq j \leq n_g$ and the corresponding torque limits:

$$\lambda_s(\alpha^*_{k+i|k-1}, \alpha^j_{k+i|k})\, T^{ts}_{ice,k+i|k} \leq T_{ice,max}(\alpha^j_{k+i|k}) \tag{55}$$

$$\lambda_s(\alpha^*_{k+i|k-1}, \alpha^j_{k+i|k})\, T^{ts}_{ice,k+i|k} \geq T_{ice,min}(\alpha^j_{k+i|k}) \tag{56}$$

$$\lambda_s(\alpha^*_{k+i|k-1}, \alpha^j_{k+i|k})\, T^{ts}_{em,k+i|k} \leq T_{em,max}(\alpha^j_{k+i|k}) \tag{57}$$

$$\lambda_s(\alpha^*_{k+i|k-1}, \alpha^j_{k+i|k})\, T^{ts}_{em,k+i|k} \geq T_{em,min}(\alpha^j_{k+i|k}) \tag{58}$$

for $0 \leq i \leq H_u - 1$ hold. Here, λ_s denotes the torque scaling factor as introduced in (46), $\alpha^*_{k+i|k-1}$ the optimal gear choice determined at time $k-1$ for time step $k+i$ of the control horizon and $T^{ts}_{ice/em,k+i|k}$ the optimal machine torque for the corresponding time step (provided by the torque split MPC). Through the validation of the inequalities (51)-(58) an admissible set of relaxed controls is determined a priori. If the gear $\alpha^j_{k+i|k}$ is not feasible at time step $k+i$ the corresponding relaxation variable $\alpha_{j,k+i|k}$ is set to zero. The resulting optimization problem (47)-(50) is finally stated as QP problem which can be solved efficiently obtaining a sequence of relaxed controls $\alpha^*_k = [\alpha^*_{k|k}, \ldots, \alpha^*_{k+H_u-1|k}]$.

4) Rounding of Relaxed Optimal Solution: Finally, a rounding strategy is applied to construct an integer feasible sequence from the relaxed optimal one. Thereby as the relaxed solution is imposed under SOS-1 constraints which result from the outer convexification, the rounding strategy has to assure that the rounded solution does not violate the SOS-1 property constraint. To understand the underlying rounding concept, lets assume that two control functions are assigned a value of 0.5 while the others are zero. A simple rounding might cause that two control functions are rounded to one, thus obviously violating the SOS-1 constraint. To overcome this issue, we apply a rounding scheme that has been proposed in [12]. Particularly, let $\hat{\alpha}_{j,k+i|k}$ denote the rounded, i.e., integer counterpart of $\alpha_{j,k+i|k}$. To obtain the rounded solution at time $k+i$, [9], [12] propose to first sum up the integer solutions $\hat{\alpha}_j$ up to the preceding time step $k+i-1$ and subtract the result from the sum of fractional solutions α_j up to the current time step $k+i$, i.e.,

$$\hat{\beta}_{j,k+i} = \sum_{m=0}^{i} \alpha_{j,k+m} - \sum_{m=0}^{i-1} \hat{\alpha}_{j,k+m}. \tag{59}$$

The selected gear j at time $k+i$ is finally determined by choosing the smallest gear with the largest value $\hat{\beta}_{j,k+i}$:

$$\hat{\alpha}_{j,k+i|k} = \begin{cases} 1 & \text{if } \hat{\beta}_{j,k+i} \geq \hat{\beta}_{l,k+i} \ \forall l \neq j \\ & \wedge\ j < l \ \forall l : \hat{\beta}_{j,k+i} = \hat{\beta}_{l,k+i} \\ 0 & \text{else} \end{cases} \tag{60}$$

The rounding strategy (59)-(60), denoted as Sum Up SOS-1 Rounding, is specifically tailored to the special ordered set restrictions that stem from the outer convexification. A proof that this strategy preserves the fulfillment of SOS-1 constraints can be found in [13].

V. Simulation Results

A. Simulation Setup

The performance of the introduced distributed MPC approach is assessed on a real-world driving cycle, i.e., a cycle recorded in a real vehicle in the area of Aachen, Germany comprised of urban, inter-urban and highway parts. We compare the centralized mixed-integer MPC (abbreviated as MIMPC, see section III) with the distributed MPC (abbreviated as DMPC, see section IV) approach to assess the optimality and computational effort of the DMPC solution with respect to MIMPC. For both controllers, we apply a sample time of $T_s = 1\,\mathrm{s}$. To solve the MIMPC problem, CPLEX *cplexmiqp* [15] is employed as mixed-integer QP solver while qpOASES [16] is used to obtain the solution of the QP problems for DMPC. Both controllers are parametrized equally for the purpose of an appropriate comparison: $q^{ts}_{\dot{m}_f} = q^{gs}_{\dot{m}_f} = q_{\dot{m}_f} = 1$, $q^{ts}_{SoC} = q^{gs}_{SoC} = q_{SoC} = 300$, $r^{ts}_{\Delta T_{ice}} = r_{\Delta T_{ice}} = 10^{-3}$, $r^{ts}_{\Delta T_{br}} = r_{\Delta T_{br}} = 0$, $r^{gs}_{\Delta\alpha^j} = r_{\Delta\gamma^j} = 2 \cdot 10^{-1}$, $s^{ts}_{T_{ice}} = s_{T_{ice}} = 0$, $s^{ts}_{T_{br}} = s_{T_{br}} = 1$ and $\rho_s = 10^5$. The battery reference value is set to $60\,\%$ of its charge ($SoC_{ref} = 0.6$), while the limits are assumed to be defined as: $SoC_{min} = 0.5$ and $SoC_{max} = 0.7$ respectively. The prediction and control horizon in the MPC schemes are selected as $H_u = H_p = 10$.

B. Results

Simulation results in Fig. 2 indicate that the overall behavior of both strategies is quite similar. As far as the controlled outputs are concerned, DMPC depletes the battery slightly less than MIMPC resulting in a higher final SoC and higher fuel consumption compared to MIMPC. At the same time, the corresponding trajectories of the controlled

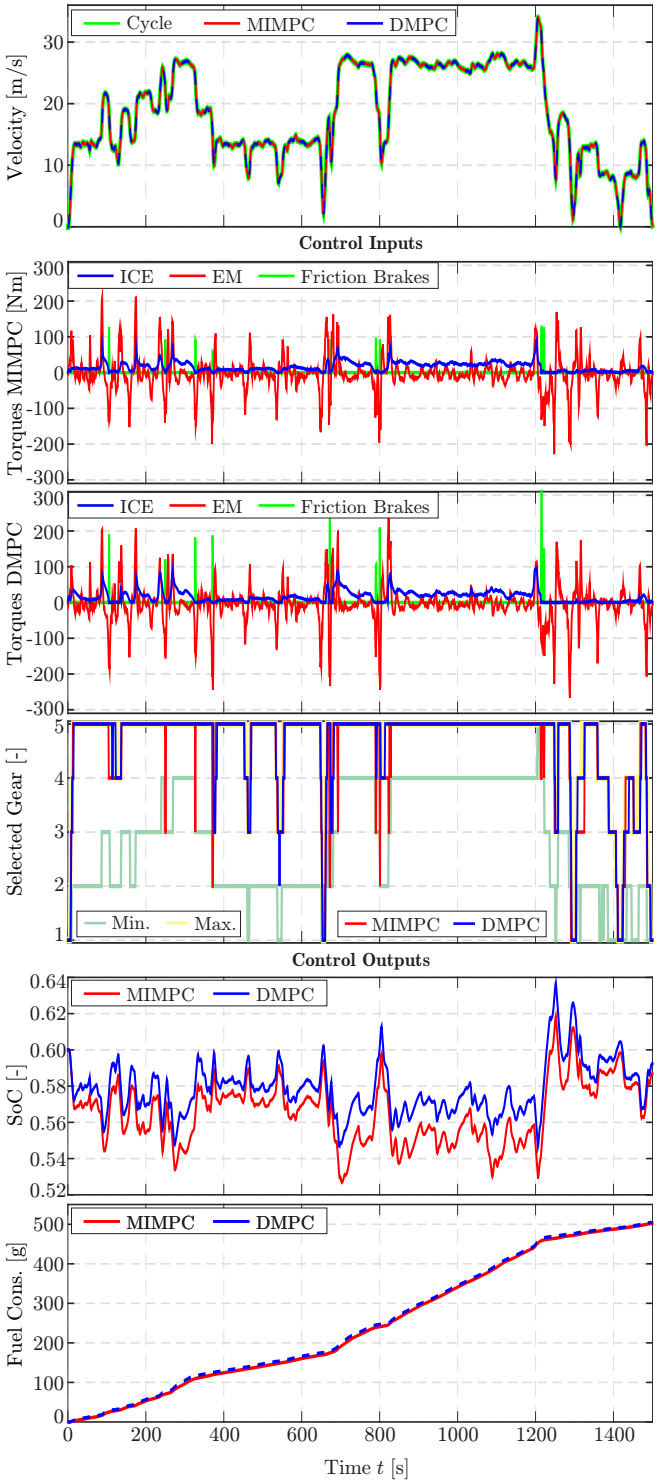

Fig. 2. Simulation results on a real-world driving cycle

outputs show the same qualitative behavior while having an offset to each other. The particular results are summarized in Tab. I. Considering the equivalent fuel consumption, we can conclude that MIMPC and DMPC achieve a similar performance regarding fuel efficiency. The application of DMPC controller leads to $0.49\,\%$ higher fuel consumption than the application of the MIMPC. However the SoC value at the end of the driving is closer to the reference value by the DMPC controller, i.e., it is $0.85\,\%$ higher than than of the MIMPC so that the DMPC shows slightly better charge sustainability. Analyzing the control inputs, it can be recognized that the use of the ICE is almost equal for MIMPC and DMPC while the friction brakes are employed more extensively for DMPC. The reason of this behavior can be understood when investigating the gear choice of MIMPC compared to DMPC. Although, the gear choice is equal most of the time, we can see quite short time intervals in which MIMPC selects a lower gear than DMPC. In these situations, the maximum ability to recover energy through regenerative braking is reached such that the friction brakes have to be utilized. Here, MIMPC decides to select a lower gear to recover a higher amount of energy through regenerative braking and thus to waste less energy in heat by engaging the friction brakes less. Although this behavior is optimal from a mathematical point of view, such a frequent shifting should be avoided in an actual vehicle. This can actually been done in two different ways. First, the gear choice could be forwarded to the vehicle with a hysteresis in time or, second, the cost functional might be further extended to avoid such situations. The latter aspect will be part of future work. The CPU computation time reported in Table II is obtained from simulations on a Lenovo T430 with 2.6 GHz IntelCore i5 vPro processor and MATLAB 2014b. Applying the distributed cooperative MPC approach the computational effort is significantly reduced compared to the execution time of the centralized MPC controller. The computation time in the DMPC is sufficiently smaller than the controller sampling rate $T_s = 1\,\mathrm{s}$ which is commonly used as sampling rate of HEV energy management strategies [17]. This enables further evaluation of the proposed distributed EMS on a rapid control prototyping hardware.

TABLE I

FUEL ECONOMY OF THE MIMPC AND DMPC APPROACH

	Fuel cons. [g]	Final SoC [-]	SoC gain/loss [%]
MIMPC	502.16	0.587	-2.20
DMPC	504.62	0.592	-1.33

TABLE II

COMPUTATIONAL COMPLEXITY OF PROPOSED EMS APPROACHES

	MIMPC	DMPC	
		Torque Split	Gear Shifting
Min. execution time	106.6 ms	2.8 ms	4.7 ms
Max. execution time	5263 ms	5.8 ms	16.1 ms
Mean. execution time	171.3 ms	3.8 ms	7 ms

VI. CONCLUSION

In series production passenger vehicles, control architectures are rather distributed than centralized, i.e., control algorithms are executed on separate interconnected ECUs.

Considering the energy management of hybrid electric vehicles, the torque split between the propulsion machines is determined by a hybrid energy management ECU while gear shifts are usually optimized by a gearbox ECU. Therefore, we proposed a distributed cooperative control architecture in which one MPC controller determines the torque distribution while the other optimizes the gear switching over the examined driving cycle. The controllers are designed to optimize the fuel economy of the HEV system. The performance of the proposed control scheme is assessed with regards to the performance of the centralized MPC scheme. To design both, the distributed and centralized MPC control approach, partial convexification and relaxation are applied which enables significant reduction of the computation time. The simulation results indicate that the DMPC achieves almost the same fuel economy as MIMPC, while at the same time the computational effort is reduced significantly. Future work will address the evaluation of the DMPC approach on a rapid control prototyping platform.

REFERENCES

[1] C. Musardo, G. Rizzoni, and B. Staccia, "A-ECMS: An adaptive algorithm for hybrid electric vehicle energy management," in *44th IEEE CDC-ECC*, 2005, pp. 1816–1823.

[2] H. Borhan, A. Vahidi, A. Phillips, M. Kuang, I. Kolmanovsky, and S. Di Cairano, "MPC-based energy management of a power-split hybrid electric vehicle," *IEEE Transactions on Control Systems Technology*, vol. 20, no. 3, pp. 593–603, 2012.

[3] D. Opila, X. Wang, R. McGee, R. Gillespie, J. Cook, and J. Grizzle, "An energy management controller to optimally trade off fuel economy and drivability for hybrid vehicles," *IEEE Transactions on Control Systems Technology*, vol. 20, no. 6, pp. 1490–1505, 2012.

[4] V. Ngo, T. Hofman, M. Steinbuch, and A. Serrarens, "Optimal control of the gearshift command for hybrid electric vehicles," *Vehicular Technology, IEEE Transactions on*, 2012.

[5] M. Joševski and D. Abel, "Multi-time Scale Model Predictive Control Framework for Energy Management of Hybrid Electric Vehicles," in *IEEE Conference on Decision and Control*, 2014.

[6] J. Liu and H. Peng, "Modeling and control of a power-split hybrid vehicle," *IEEE Transactions on Control Systems Technology*, vol. 16, no. 6, pp. 1242–1251, 2008.

[7] V. van Reeven, T. Hofman, R. Huisman, and M. Steinbuch, "Extending energy management in hybrid electric vehicles with explicit control of gear shifting and start-stop," in *American Control Conference (ACC), 2012*, 2012.

[8] C. Kirches, "Fast numerical methods for mixed-integer nonlinear model-predictive control," Ph.D. dissertation, Ruprecht-Karls-Universität Heidelberg, 2010.

[9] S. Sager, *Numerical methods for mixed–integer optimal control problems*. Der andere Verlag, 2005. [Online]. Available: http://mathopt.de/PUBLICATIONS/Sager2005.pdf

[10] K. Wipke, M. Cuddy, and S. Burch, "Advisor 2.1: a user-friendly advanced powertrain simulation using a combined backward/forward approach," *IEEE Transactions on Vehicular Technology*, vol. 48, no. 6, pp. 1751–1761, 1999.

[11] L. Guzzella and A. Sciaretta, *Vehicle Propulsion Systems*. Springer, 2013.

[12] M. Jung, "Relaxations and approximations for mixed-integer optimal control," Ph.D. dissertation, 2013.

[13] S. Sager, "On the Integration of Optimization Approaches for Mixed-Integer Nonlinear Optimal Control," University of Heidelberg, 2011, habilitation. [Online]. Available: http://mathopt.de/PUBLICATIONS/Sager2011d.pdf

[14] M. Jung, C. Kirches, and S. Sager, "On Perspective Functions and Vanishing Constraints in Mixed-Integer Nonlinear Optimal Control," in *Facets of Combinatorial Optimization – Festschrift for Martin Grötschel*. Springer Berlin Heidelberg, 2013, pp. 387–417. [Online]. Available: http://www.mathopt.de/PUBLICATIONS/Jung2013.pdf

[15] ILOG, Inc, "ILOG CPLEX: High-performance software for for linear programming, mixed integer programming, and quadratic programming," 2015, see http://www.ilog.com/products/cplex/.

[16] H. J. Ferreau, "qpOASES User's Manual (Version 3.0beta)," *Optimization in Engineering Center (OPTEC) and Department of Electrical Engineering, KU Leuven*, 2012.

[17] S. Cairano, D. Bernardini, A. Bemporad, and I. Kolmanovsky, "Stochastic mpc with learning for driver-predictive vehicle control and its application to hev energy management," *IEEE Transactions on Control Systems Technology,*, vol. PP, no. 99, pp. 1–1, 2013.